ISSN 1573-160X, *PHYSICAL OCEANOGRAPHY*, Vol. 32, Iss. 4, pp. 524-536 (2025)
Original Russian Text © V. V. Efimov, D. A. Iarovaia, 2025,
published in *Morskoy Gidrofizicheskiy Zhurnal*, 2025, Vol. 41, Iss. 4, pp. 501–514

Original article

Numerical Modeling of Cold Air Intrusion in the Crimean Region on January 22–24, 2010

V. V. Efimov ✉, D. A. Iarovaia

Marine Hydrophysical Institute of RAS, Sevastopol, Russian Federation
✉ *vefim38@mail.ru*

Abstract
Purpose. The purpose of the work is to numerically investigate the response of near-surface marine and atmospheric fields in the Crimean region to the cold air intrusion in January 22−24, 2010.
Methods and Results. A coupled mesoscale sea–atmosphere model NOW (NEMO-OASIS-WRF) with a 1 km resolution was used. The interaction of incoming airflow with the Crimean Mountains during the cold intrusion was reproduced, as well as the main changes in near-surface atmospheric and marine fields that occurred in the region of the Southern coast of Crimea during the cold air intrusion were analyzed. It is shown that the cold intrusion was characterized by a northeasterly wind throughout the region with maximum speeds up to 10 m/s over the land and up to 20 m/s over the sea. The sea surface temperature in the region decreased mainly by ~ 0.5 °C. To the south of peninsula, in the Rim Current area, a local decrease in sea surface temperature constituted ~ −1.5 … −1 °C. A distinctive feature of the considered case was a small thickness (less than 1 km) of the cold airflow incoming to the Crimean Mountains. On the over-land atmospheric profiles corresponding to the foothill region, a relatively thin cold surface layer with the increased wind speed and high values of stability frequency at its upper boundary is clearly pronounced.
Conclusions. Despite their short duration, winter intrusions of cold air across the northern boundary of the Black Sea region induce significant regional disturbances in the atmospheric and marine fields. The sea responds to cold air intrusions with a decrease in sea surface temperature, which can be explained by strong fluxes of sensible and latent heat from the sea surface, as well as by the entrainment processes at the lower boundary of the upper mixed layer. To the south of the Crimean Peninsula, there is an additional factor contributing to temperature decrease, namely the transport of colder water from the open sea towards the coast, which develops in response to the strengthening of along-coastal northeasterly winds over the sea. In the atmosphere, at its lower levels, the incoming cold flow is blocked by the coastal Crimean Mountains. As a result, the descending compensatory flows arise over the leeward slope of the mountains that leads to an increase in near-surface air temperature at the Southern coast of Crimea. Another consequence of the blocking is the absence of a cold gravity flow on the leeward slope of the Crimean Mountains, unlike other cases of cold air intrusions, such as the Yalta bora event in December 2013.

Keywords: mesoscale coupled modeling, cold air intrusion, Crimea region, near-surface current velocity fields in the sea, near-surface temperature fields in the sea, Black Sea

Acknowledgements: The study was conducted as part of the state assignment (No. FNNN-2024-0014).

For citation: Efimov, V.V. and Iarovaia, D.A., 2025. Numerical Modeling of Cold Air Intrusion in the Crimean Region on January 22–24, 2010. *Physical Oceanography*, 32(4), pp. 524-536.

Introduction

A notable feature of the local air circulation in the Black Sea region is the occurrence of cold air intrusion (CAI) during winter across the region's northern boundary into the atmospheric boundary layer over the sea. This extreme weather phenomenon is accompanied by a significant increase in surface wind speed of up to 10–15 m/s and a decrease in near-surface air temperature down to −10 … −15 °C [1]. At the same time, the sea surface temperature is approximately + 9 °C. Consequently, intense cloud convection develops over the sea, appearing on satellite images as cloud "streets" (Fig. 1).

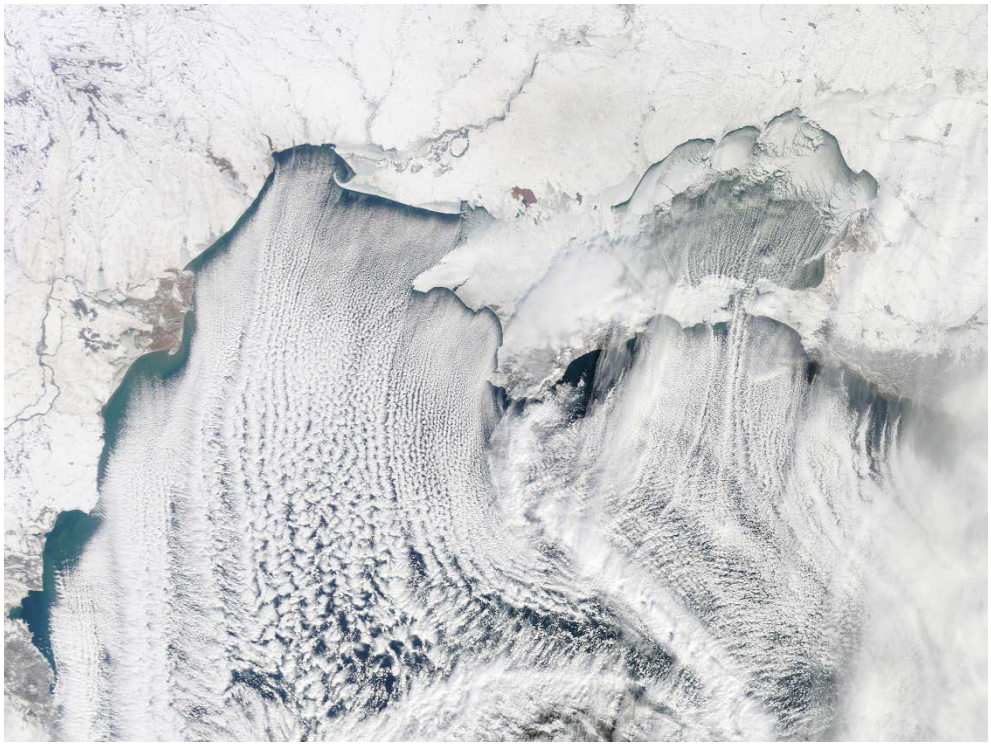

F i g. 1. Snapshot of cloudiness on January 25, 2010 obtained using the MODIS spectroradiometer installed on Terra satellite. Data source is website http://rapidfire.sci.gsfc.nasa.gov

Episodes of cold intrusions in the Black Sea region are mainly caused by winds from the north and northeast. There are two types of synoptic situations that lead to extreme cooling of the Black Sea during autumn and winter periods. Most often, an intense anticyclone is located north of the Black Sea. On the southeastern periphery of the anticyclone, a northeasterly flow of cold air forms, accompanied by high surface wind speeds [2]. In other cases, there is a less intense anticyclone north of the Black Sea and a cyclone to the south, centered in Asia Minor. The airflow on the southeastern periphery of the anticyclone increases due to the flow on the northwestern periphery of the cyclone, creating an intense Novorossiysk bora. This frontal-type bora is most frequent during the cold season when conditions for

the development of a true bora are met: wind speeds of at least 15 m/s and near-surface air temperatures no higher than – 10 °C [2, 3].

Relatively short-lived (usually no more than 2−3 days) but intense cold intrusions result in changes to the characteristics of the marine environment that stand out well against the background of synoptic variability. It should be noted that the cooling of the upper sea layer during cold intrusions occurs due to heat loss from the surface; however, the mixing of the upper layer has a different, non-convective physical mechanism. Interaction processes in the sea-atmosphere system for a characteristic CAI case were described in [4] using the coupled NEMO-WRF numerical model. Since cold intrusions are characterized by both low air temperatures and high surface wind speeds, a convective type of circulation (such as cellular convection in the atmospheric marine boundary layer) does not usually develop in the sea. Deep penetrating cooling of the upper sea layer during cold intrusions is mainly associated with turbulent mixing caused by the shear instability of currents and wind wave breaking [4]. Cold intrusions that recur during winter periods can influence the formation of the cold intermediate layer (CIL) in the Black Sea by determining the temperature of the surface layer at the end of seasonal winter cooling [4]. During these cold episodes, the upper quasi-homogeneous layer (UQL) can significantly deepen, merging with the CIL[1].

In addition to the general decrease in the sea surface temperature, which is most pronounced in the northern coastal region, specific local features appear in some areas of the sea during CAI. One such region is the northeastern area, where the Novorossiysk bora develops and leaves a significant mark on the temperature and velocity fields of the atmosphere and the sea [8, 9]. The second region where CAI causes specific disturbances in the boundary layers of the atmosphere and the sea is the Crimean region, where the influence of the relatively high Crimean Mountains is significant. During the autumn-winter period when cold air intrusions occur, the Yalta bora can develop in the Southern coast of Crimea (SCC), similar to the Novorossiysk bora [10]. Furthermore, the entire lower tropospheric circulation and, consequently, the temperature field south of the SCC are significantly influenced by the Crimean Mountains [11].

This paper uses the coupled sea-atmosphere NEMO-WRF numerical model to examine features of the temperature, wind speed, and surface current fields in the Crimean region during CAIs, taking the event of January 22–24, 2010 as an example (Fig. 1). This event has been previously studied in our works [1, 4]. Using the WRF atmospheric model, the structure of the convective atmospheric boundary layer over the western part of the sea on January 25, 2010, was reproduced. It was shown that convection occurred under quasi-stationary but substantially heterogeneous spatial conditions [1]. The convective cells in the atmosphere provided large fluxes of sensible and latent heat from the sea surface (up to 1000 W/m² in the northwest), which led to the rapid cooling of the sea surface layer by 1−2 °C [4].

[1] Blatov, A.S., Bulgakov, N.P., Ivanov, V.A., Kosarev, A.N. and Tuljulkin, V.S., 1984. *Variability of the Black Sea Hydrophysical Fields*. Leningrad: Gidrometeoizdat, 240 p. (in Russian).

This work aims to investigate the response of marine and atmospheric fields in the Crimean region to a characteristic case of CAI using a coupled mesoscale model.

Numerical model

The coupled sea-atmosphere model (NOW) [12] consists of the NEMO ocean model [2], the WRF non-hydrostatic atmospheric model [3], and the OASIS coupler (an application that handles data exchange between NEMO and WRF). The simulation used two computational grids: one with 3 km resolution covering all three seas (the Black Sea, the Azov Sea, and the Marmara Sea), and one nested grid with 1 km resolution covering the area (30−36°E; 43–47°N). The simulation results with 1 km resolution are considered further in the work.

The NOW model has been described in previous works (see, for example, [4]), so here we will only note that in the NEMO model, the GLS k-ε scheme [13] was used for parameterizing turbulent exchange. In this scheme, the exchange coefficients are defined as a function of two prognostic variables: turbulent kinetic energy k and turbulent kinetic energy dissipation rate ε. Additionally, the NEMO model accounts for surface wave breaking. To accomplish this, the following boundary condition is used: at the sea surface, the k and ε values are calculated as a function of wind stress.

Regional changes in velocity and temperature fields

Changes in parameters of the upper sea layer. Fig. 1 shows a satellite image of the studied CAI case. Over the western half of the sea, it is clearly visible that the cloud field consists of elongated cloud “streets” aligned with the northerly wind direction. The horizontal size of the cloud structures significantly increases with distance from the windward shore (from 1–2 km near the shore to ~ 10 km at a distance of 300 km from the shore). This is a characteristic feature of cloud fields that form during CAI [14].

Fig. 2 shows the temporal changes in surface wind speed and surface air temperature at the 34°E, 45°N point, which is located in the flat central part of Crimea. The CAI event itself, which lasted about two days (from the second half of January 22 to the first half of January 24), is well represented by increased wind speeds and a significant decrease in surface air temperature.

Fig. 3, a shows the surface wind speed and current velocity fields at 12:00 on January 23, when the wind speed over land was greatest. This cold air intrusion is characterized by northeasterly winds throughout the Crimean region, with maximum speeds of up to 10 m/s over land and up to 20 m/s over the sea. A significant aspect of water circulation in the Black Sea is the Black Sea Rim Current (RC), a year-round cyclonic alongshore current that reaches maximum intensity in late winter [15]. Large current velocities of up to 0.8 m/s are associated with the RC at a distance

[2] Skamarock, W.C., Klemp, J.B., Jimy, D., Gill, D.O., Barker, D.M., Duda, M.G., Huang, X-Y., Wang, W. and Powers, J.G., 2008. *A Description of the Advanced Research WRF Version 3. NCAR Technical Note*. NCAR/TN-475+STR, 113 p. https://doi.org/10.13140/RG.2.1.2310.6645

[3] NEMO Team, 2016. *NEMO Ocean Engine*. Note du Pôle de Modélisation de l'Institut Pierre-Simon Laplace, No. 27. France: IPSL, 412 p. https://doi.org/10.5281/zenodo.3248739

of 50−70 km south of Crimea. The response of the upper sea layer to the cold intrusion is also shown. This is evidenced by the decrease in SST (Δ*sst*) during the intrusion period from 12:00 on January 22 to 12:00 on January 24. Outside the RC area, Δ*sst* was ~ −0.5 °C except for coastal areas. Assuming the UQL thickness is 40 m, we can estimate the total (sensible + latent) heat flux $Q = \Delta sst \cdot \rho \cdot C_p \cdot H/(48\ \text{h})$, where $\rho = 1025$ kg/m³ and $C_p = 3900$ J/(kg·°C) are the density and specific heat capacity of seawater, respectively; H is the UQL thickness; Q is ~ 500 W/m², which is close to the modeled value.

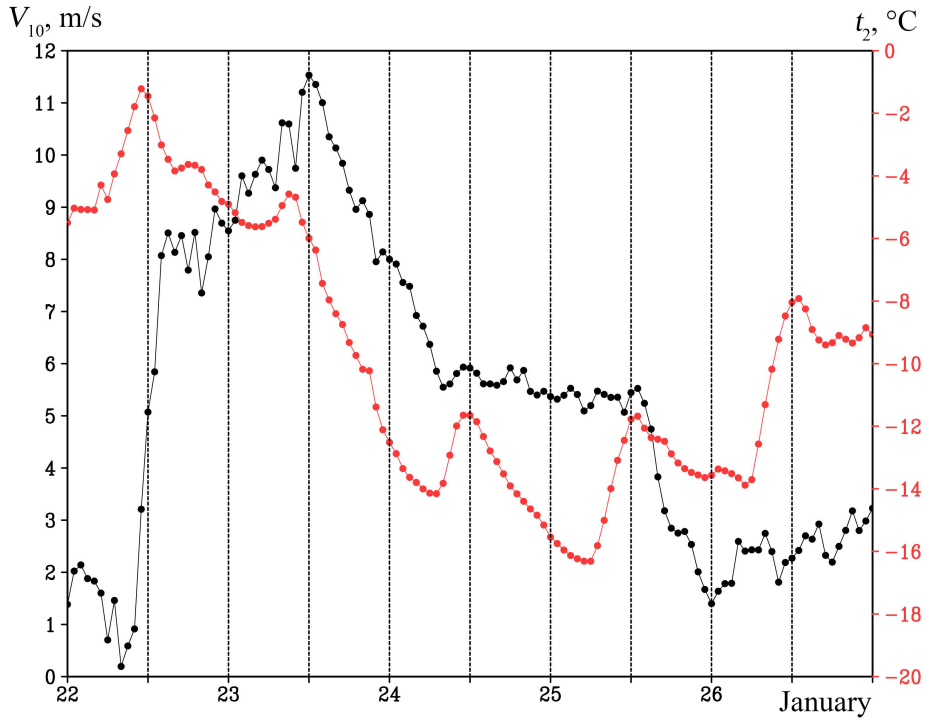

F i g. 2. Temporal variation of wind speed at the 10 m height (black curve) and air temperature at the 2 m height (red curve) at point 34°E, 45°N (point location is marked in Fig. 3, *a*)

An area of elevated negative Δ*sst* values stands out south of the peninsula, ranging from −1.5 to −1 °C. Fig. 3, *b* explains the origin of these values. This figure shows the SST field at the beginning of the cold intrusion, as well as the change in the surface current velocity field over the first 12 hours of the intrusion for a small area near the southeastern coast of Crimea. The SST field in this area exhibits strong spatial heterogeneity: relatively warm water with a temperature of 9−10 °C is found near the shore, while colder water with a temperature 1–1.5 °C lower is found farther offshore. After the CAI onset, an onshore-directed Ekman transport with velocities up to 0.2 m/s developed in the sea in response to the sharp intensification of the northeasterly alongshore wind. This led to an additional advective decrease in SST near the southeastern coast.

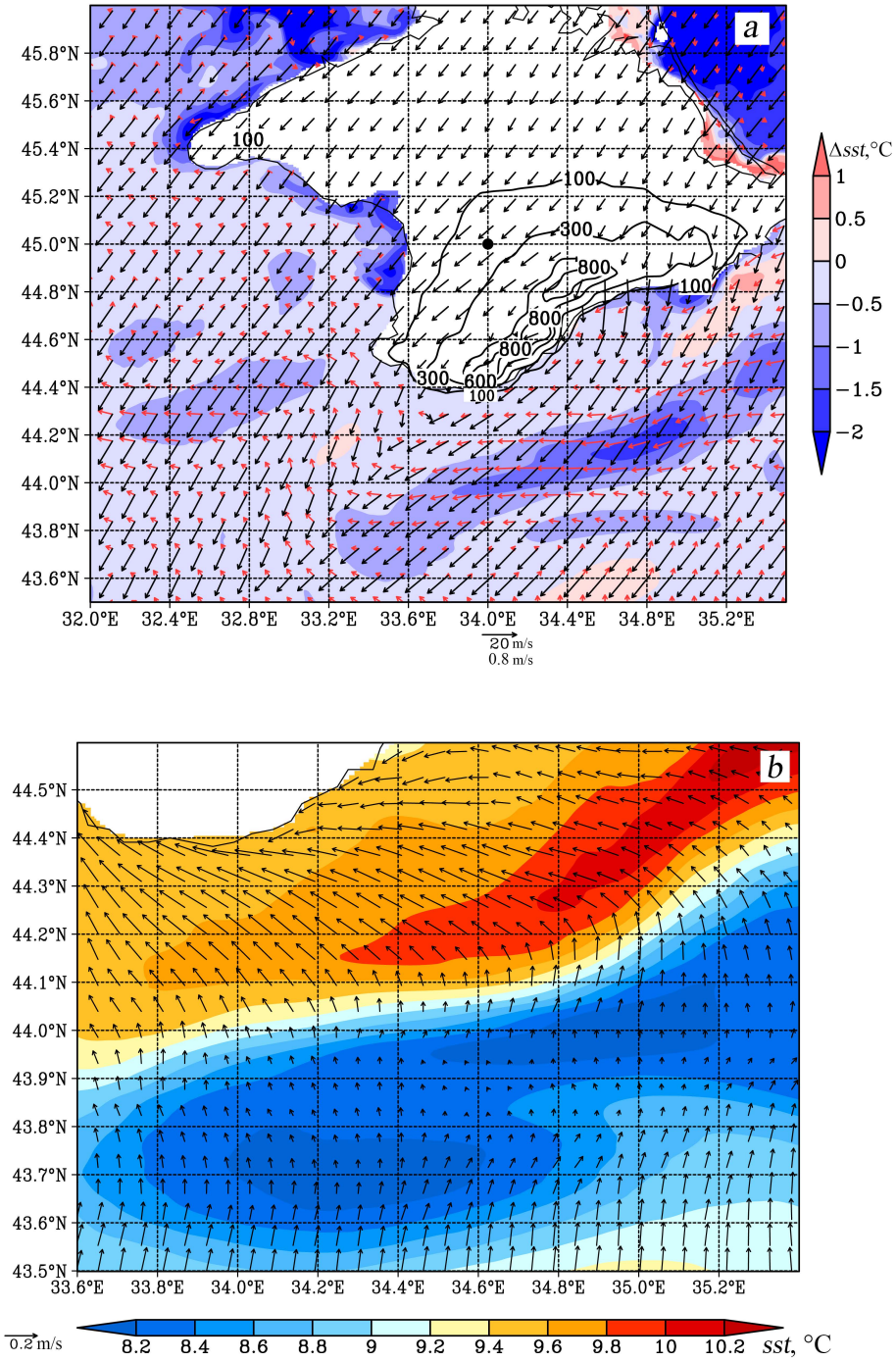

F i g. 3. Change in SST (Δ*sst*, °C) between 12:00, January 22 and 12:00, January 24, near-surface wind speed field (black arrows) and near-surface current velocity field (red arrows) at 12:00, January 23; relief height (m) is shown by isolines (*a*); SST field at 12:00, January 22, and change in the near-surface current velocity field between 12:00, January 22 and 00:00, January 23 (*b*)

Fig. 4 shows the vertical structure of the velocity and temperature fields in the sea on a meridian section at 34.55°E. It demonstrates the temperature field at the beginning of the cold intrusion and how it changes during the intrusion. There is a clear tendency for the UQL to deepen towards the shore: its thickness doubles from 30 to 60 m. The temperature decrease (Δt) in the RC area (44.0–44.3°N) reaches – 1.4 °C.

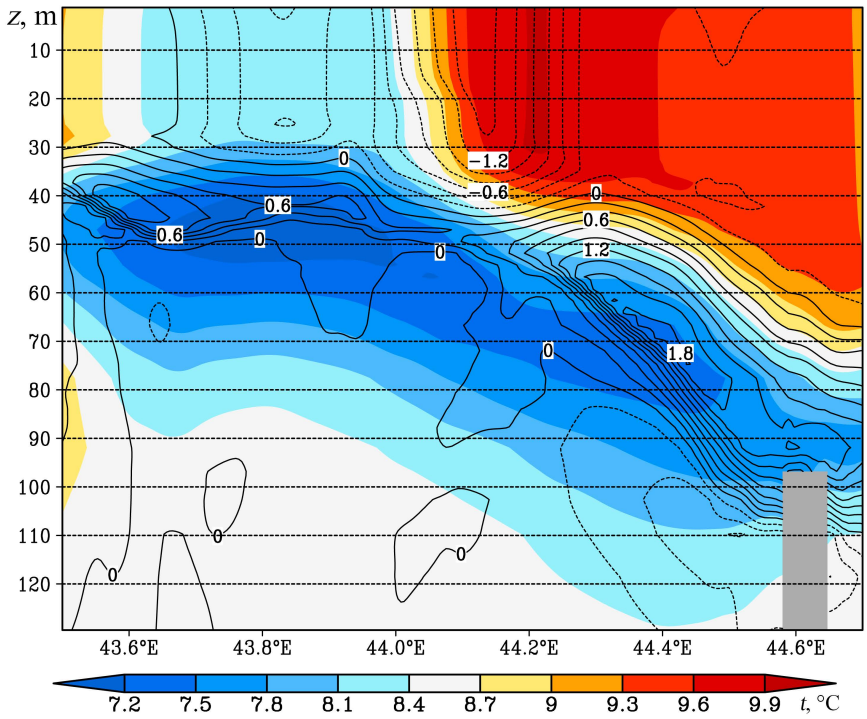

F i g. 4. Vertical structure of sea fields at meridional section along 34.55°E: sea temperature (color) at 12:00, January 22, and change in sea temperature (isolines) between 12:00, January 22 and 12:00, January 24

Fig. 5 shows the vertical temperature profiles in the upper sea layer at the beginning and end of the cold intrusion, as well as the temperature changes during the intrusion. CIL with a minimum temperature at a depth of ~ 50 m is visible. The upper sea layer response was cooling and deepening of the UQL. During the intrusion, the UQL temperature decreased by ~ 0.5 °C, and its thickness increased from 25 to 40 m. Meanwhile, the CIL thickness decreased accordingly. The physical reasons for these changes are well known: turbulent mixing of the UQL due to shear instability of currents and wind wave breaking, as well as its cooling due to sensible and latent heat fluxes from the sea surface and the entrainment of colder water from the CIL [4, 16].

Changes in atmospheric characteristics. Fig. 6 shows the surface wind speed fields at 10 m height at the beginning of the cold intrusion, as well as the change in

surface air temperature during the intrusion in the Crimean region. Note that changes in wind speed at one point in Crimea during the intrusion were shown earlier in Fig. 2. Without discussing the overall pattern of surface temperature changes related to the synoptic structure of meteorological fields, let us consider the features that are characteristic of the Crimean region. This region has sufficiently high coastal mountains that influence atmospheric and marine circulation. First, note the difference in temperature changes between the windward northwestern and leeward southeastern areas of the mountains. In the former, the air temperature decreases during cold intrusions, while in the latter, it increases. This phenomenon is associated with the physical process of a stably stratified airflow around the mountains.

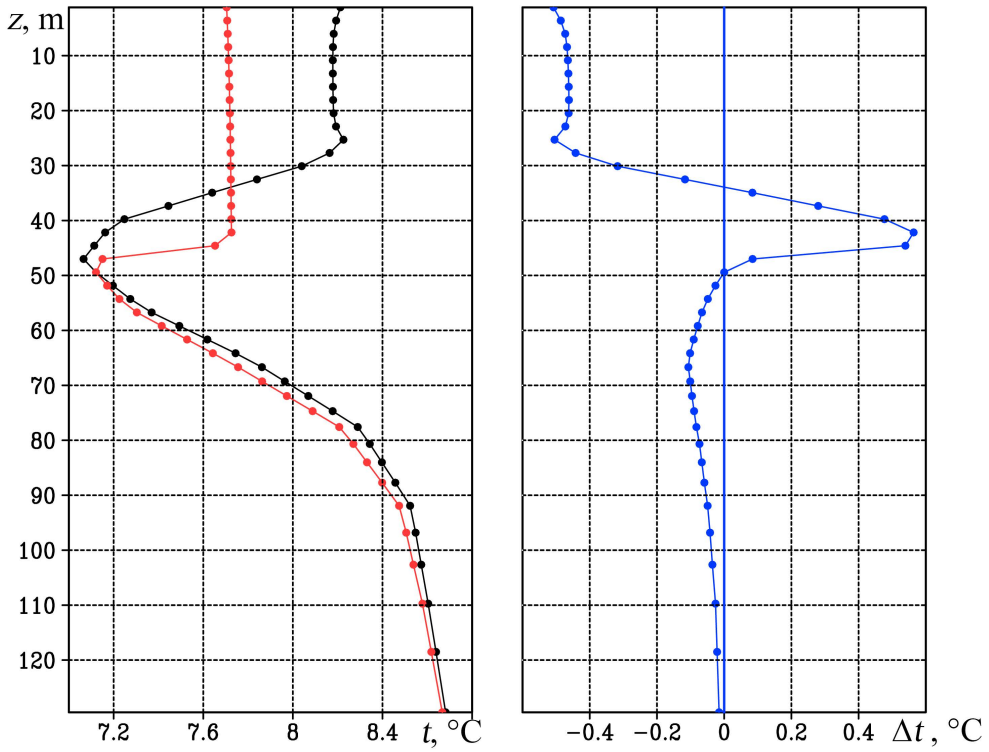

F i g. 5. Vertical profiles of sea temperature at 12:00, January 22 (black curve), 12:00, January 24 (red curve), as well as change in sea temperature (blue curve) between 12:00, January 22 and 12:00, January 24 at point (34.2°E and 43.8°N)

Fig. 7 illustrates the vertical structure of the potential temperature field and wind speed isolines on a meridional section along 34°E. The airflow mechanism around a mountainous obstacle is determined by the vertical structure of the density and flow velocity fields.

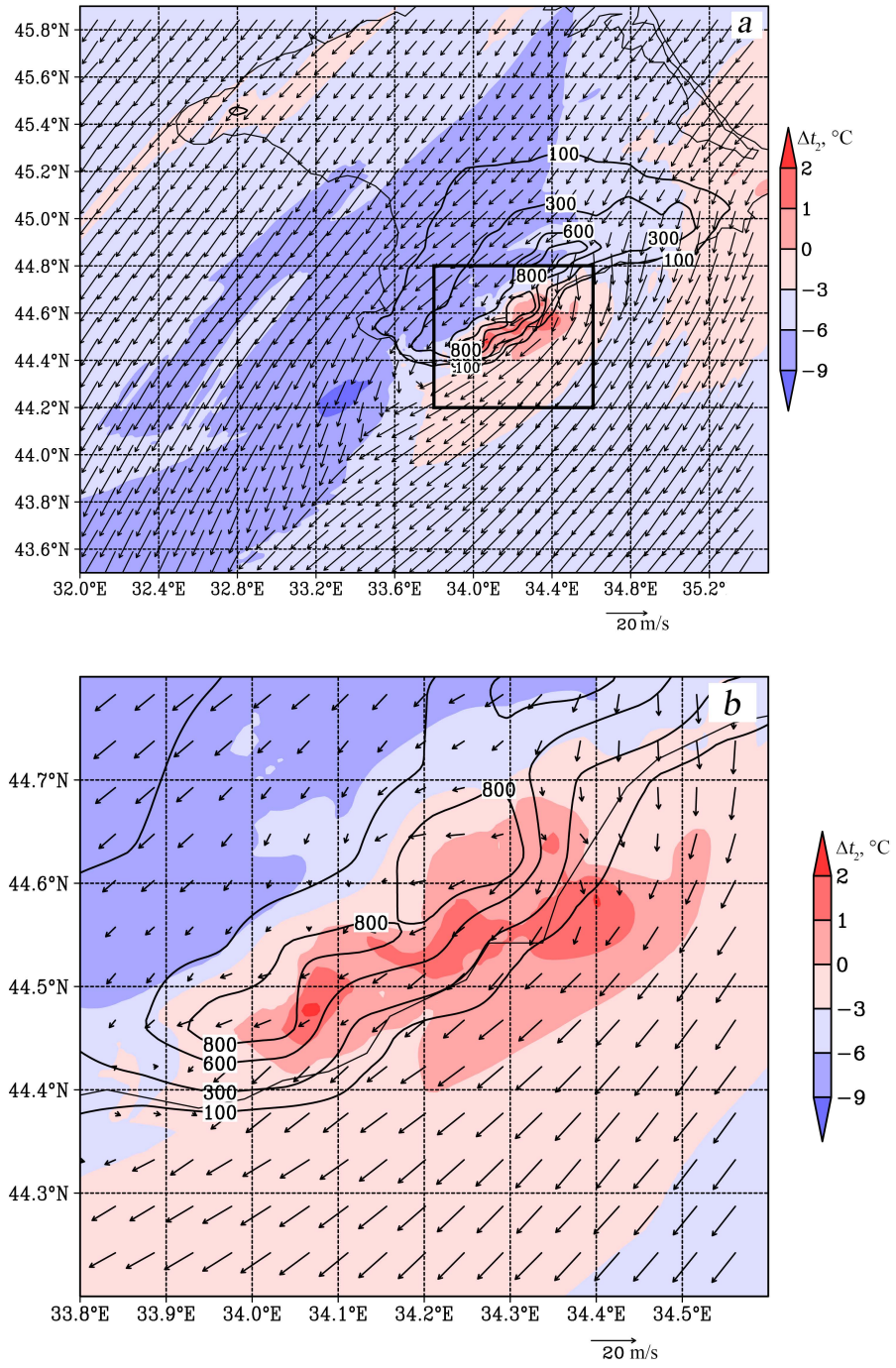

F i g. 6. Change in near-surface air temperature (Δt_2, °C) between 00:00, January 23 and 00:00, January 24, as well as near-surface wind field (black arrows) at 12:00, January 23; relief height (m) is shown by isolines (*a*); area (33.8−34.6°E, 44.2−44.8°N) highlighted by a rectangle in fragment *a*, is shown on fragment *b* on a larger scale

For our case, the vertical profiles of wind speed V and stability frequency N^2 are shown in Fig. 8. Stability frequency is equal to $(g/\rho)\cdot(\Delta\rho/\Delta z)$, where g is the acceleration due to gravity, ρ is air density, and z is height. The point in the flat land area is located at 34°E, 45°N. The most important feature of the vertical structure of the density field, and consequently the stability frequency N, determining the main properties of our intrusion case is the strong stability of the lower atmospheric layer at heights comparable to the height of the mountain ridge. The result of this is the airflow blocking effect over the windward slope of the mountains. As is well known, cold, stably stratified air flowing around a mountain ridge cannot rise above a height h equal to V/N [17, 18]. In our case, the blocking effect of cold air on the windward slope of the mountains is clearly visible as the intersection of the speed isolines with the windward slope and the concentration of cold air on the windward slope (Fig. 7). When considering velocity and temperature fields along a meridional section (such as in Fig. 7), it is necessary to consider the 3D characteristics of the mountain flow effects. The Crimean Mountain Ridge cannot be considered as a 2D obstacle because its length is only ~ 3 times greater than its width. Additionally, the wind direction is not strictly northerly and changes, albeit insignificantly, with height within the lower kilometer layer.

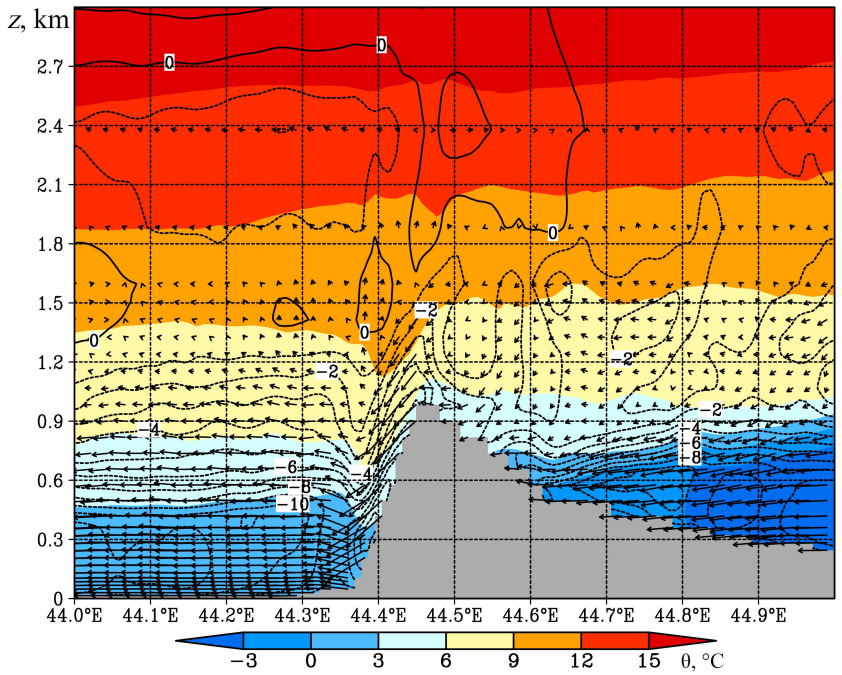

F i g. 7. Vertical structure of potential temperature θ (°C) and wind speed (m/s, isolines) fields on the meridional section along 34°E at 12:00 on January 23, 2010. Speed direction in the section plane is shown by arrows; for clarity, speed vertical component is enlarged by 10 times

Consequently, it can be concluded that the Crimean Mountains partially blocked the airflow – it went around the mountain ridge on both sides, and the northerly wind in the foothill area changed direction to northeasterly. The effect of temperature increase in the coastal area of the SCC is clearly visible in Figs. 6 and 7. Fig. 6, *b*

shows this effect as a local area of elevated surface temperature values, t_2, and low surface wind speeds. As is known, elevated potential temperature and temperature t_2 values over the leeward slope are a consequence of the mountain ridge partially blocking the airflow. This causes the surface air over the leeward slope to be replaced by potentially warmer air from higher altitudes [10]. This mechanism, which forms a local warm area over the SCC in winter, is described in [2].

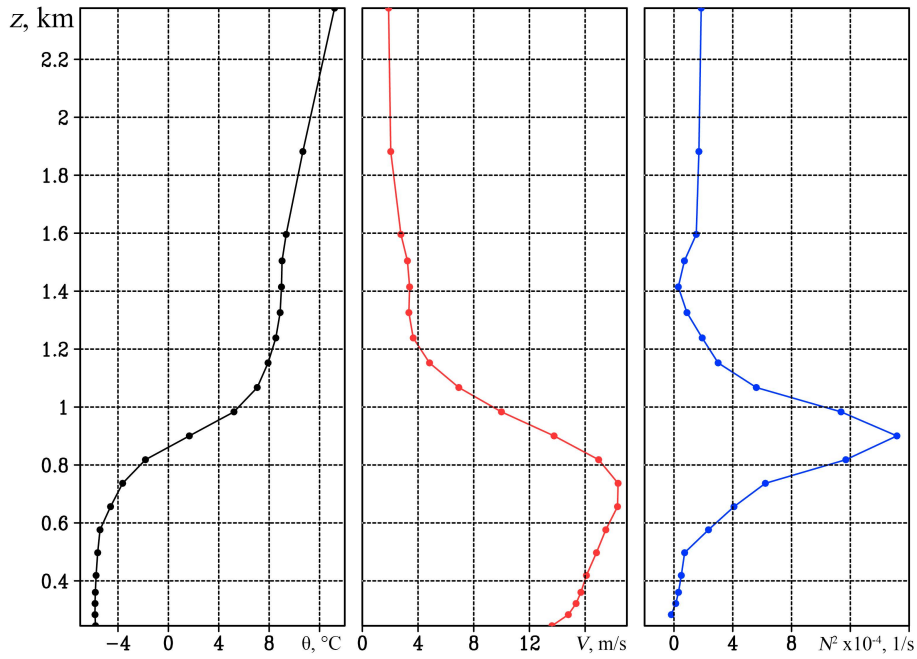

F i g. 8. Vertical profiles of potential temperature (black curve), meridional wind speed (red curve), and buoyancy frequency (blue curve) at point (34°E; 45°N) at 12:00 on January 23, 2010

Thus, a distinctive feature of the CAI event in January 2010 was the two-layer vertical structure of the troposphere, represented in Fig. 8 by the temperature and stability frequency profiles in the foothill plain part of Crimea. Anomalously cold air occupied only the lower part of the troposphere, extending up to a height of ~ 0.8 km. Above this level, wind speed decreased rapidly to a background value of 3 m/s, and stability frequency reached 0.0015 1/s. The low-tropospheric nature of the airflow distinguishes it from other CAIs in the northeastern part of the sea, which lead to the Novorossiysk bora [3] or, for example, the Yalta bora considered in [10]. Therefore, the absence of a strong downslope wind, such as a bora, in the SCC area is a distinctive feature of this intrusion in the Crimean region.

Conclusion

Despite their short duration, winter CAIs across the northern boundary of the Black Sea cause significant disturbances in atmospheric and marine fields of the region. These disturbances include strong convective instability in the atmospheric surface layer over the sea, which is visible as cloud “streets” on

satellite images, as well as sharp cooling of the upper sea layer. In some cases, CAIs can lead to the development of the Novorossiysk and Yalta bora.

This paper uses a coupled model with 1 km resolution to reproduce the interaction of the incoming air stream with the Crimean Mountains during the cold intrusion in January 2010. The main changes in the surface atmospheric and marine fields that occurred in the SCC area during the CAI were examined.

Outside the RC zone, it is shown that the decrease in SST is explained by strong fluxes of sensible and latent heat from the sea surface, as well as entrainment processes at the lower boundary of the UQL. Furthermore, south of the Crimean Peninsula, an additional factor contributing to the decrease in SST was identified: the transport of colder water from the open sea towards the shore. This phenomenon developed in response to the emergence of a strong northeasterly wind along the coast.

A distinctive feature of the considered event is the small thickness (less than 1 km) of the incoming cold airflow. Over the piedmont area, the atmospheric profiles clearly show a relatively thin cold surface layer with increased wind speed and high stability frequency values at its upper boundary. Hence, due to the incoming airflow being blocked, over the leeward slope of the Crimean Mountains and the SCC an area with a higher surface air temperature than the piedmont plain area of Crimea is formed. A gravity-driven flow, such as the Novorossiysk bora, did not reach speeds as significant as those during the CAI in December 2013.

REFERENCES

1. Efimov, V.V. and Yarovaya, D.A., 2014. Numerical Simulation of Air Convection in the Atmosphere during the Invasion of Cold Air over the Black Sea. *Izvestiya, Atmospheric and Oceanic Physics*, 50(6), pp. 610-620. https://doi.org/10.1134/S0001433814060073
2. Efimov, V.V., Savchenko, A.O. and Anisimov, A.E., 2014. Features of the Black Sea Atmosphere Heat Exchange Autumn-Winter Period. *Morskoy Gidrofizicheskiy Zhurnal*, (6), pp. 71-81 (in Russian).
3. Efimov, V.V., Komarovskaya, O.I. and Bayankina, T.M., 2019. Temporal Characteristics and Synoptic Conditions of Extreme Bora Formation in Novorossiysk. *Physical Oceanography*, 26(5), pp. 361-373. https://doi.org/10.22449/1573-160X-2019-5-361-373
4. Efimov, V.V., Yarovaya, D.A. and Komarovskaya, O.I., 2024. Deep Penetrating Cooling in the Black Sea as a Reaction to Cold Air Intrusions in Winter. *Izvestiya, Atmospheric and Oceanic Physics*, 60(5), pp. 667-679. https://doi.org/10.31857/S0002351524050081 (in Russian).
5. Piotukh, V.B., Zatsepin, A.G., Kazmin, A.S., Yakubenko, V.G., Stanichny, S.V. and Ratner, Yu.B., 2009. Impact of the Winter Atmospheric Forcing on the Variability of the Active Layer's Thermohaline Structure in the Black Sea. *Sovremennye Problemy Distantsionnogo Zondirovaniya Zemli iz Kosmosa*, 6(1), pp. 442-450 (in Russian).
6. Bayankina, T.M., Sizov, A.A. and Jurovskij, A.V., 2017. On the Role of Cold Invasion in the Formation of the Black Sea Winter Surface Temperature Anomaly. *Processes in GeoMedia*, (3), pp. 565-572 (in Russian).
7. Sizov, A.A. and Bayankina, T.M., 2019. Peculiarities of the Settling Temperature in the Upper Water Layer of the Black Sea during Invasions of Cold Air. *Doklady Earth Sciences*, 487(2), pp. 939-942. https://doi.org/10.1134/S1028334X19080105
8. Gavrikov, A.V. and Ivanov, A.Yu., 2015. Anomalously Strong Bora over the Black Sea: Observations from Space and Numerical Modeling. *Izvestiya, Atmospheric and Oceanic Physics*, 51(5), pp. 546-556. https://doi.org/10.1134/S0001433815050059
9. Ivanov, A.Yu., 2008. Novorossiysk Bora: A View from Space. *Issledovanie Zemli iz Kosmosa*, (2), pp. 68-83 (in Russian).

10. Efimov, V.V. and Komarovskaya, O.I., 2015. Spatial-Temporal Structure of Bora in Yalta. *Physical Oceanography*, (3), pp. 3-14. https://doi.org/10.22449/0233-7584-2015-3-3-14

11. Efimov, V.V. and Komarovskaya, O.I., 2019. Disturbances in the Wind Speed Fields Due to the Crimean Mountains. *Physical Oceanography*, 26(2), pp. 123-134. https://doi.org/10.22449/1573-160X-2019-2-123-134

12. Samson, G., Masson, S., Lengaigne, M., Keerthi, M.G., Vialard, J., Pous, S., Madec, G., Jourdain, N.C., Jullien, S. [et al.], 2014. The NOW Regional Coupled Model: Application to the Tropical Indian Ocean Climate and Tropical Cyclone Activity. *Journal of Advances in Modeling Earth Systems*, 6(3), pp. 700-722. https://doi.org/10.1002/2014ms000324

13. Umlauf, L. and Burchard, H., 2003. A Generic Length-Scale Equation for Geophysical Turbulence Models. *Journal of Marine Research*, 61(2), pp. 235-265. https://doi.org/10.1357/002224003322005087

14. Melfi, S.H. and Palm, S.P., 2012. Estimating the Orientation and Spacing of Midlatitude Linear Convective Boundary Layer Features: Cloud Streets. *Journal of the Atmospheric Sciences*, 69(1), pp. 352-364. https://doi.org/10.1175/jas-d-11-070.1

15. Ivanov, V.A. and Belokopytov, V.N., 2013. *Oceanography of the Black Sea*. Sevastopol: MHI, 210 p. (in Russian).

16. Zatsepin, A.G., Kremenetskiy, V.V., Piotukh, V.B., Poyarkov, S.G., Ratner, Yu.B., Soloviev, D.M., Stanichnaya, R.R., Stanichny, S.V. and Yakubenko, V.G., 2008. Formation of the Coastal Current in the Black Sea Caused by Spatially Inhomogeneous Wind Forcing upon the Upper Quasi-Homogeneous Layer. *Oceanology*, 48(2), pp. 159-174. https://doi.org/10.1134/S0001437008020021

17. Gill, A.E., 1982. *Atmosphere-Ocean Dynamics*. International Geophysics Series, vol. 30. New York: Academic Press, 662 p.

18. Lin, Y.-L., 2007. *Mesoscale Dynamics*. Cambridge: Cambridge University Press, 630 p. https://doi.org/10.1017/CBO9780511619649

Submitted 11.10.2024; approved after review 03.03.2025;
accepted for publication 15.05.2025.

About the authors:
Vladimir V. Efimov, Head of Atmosphere-Ocean Interaction Department, Marine Hydrophysical Institute of RAS (2 Kapitanskaya Str., Sevastopol, 299011, Russian Federation), DSc. (Phys.-Math), Professor, **SPIN-code: 4902-8602**, **ResearcherID: P-2063-2017**, **Scopus Author ID: 6602381894**, vefim38@mail.ru

Darya A. Iarovaia, Leading Researcher, Marine Hydrophysical Institute of RAS (2 Kapitanskaya Str., Sevastopol, 299011, Russian Federation), CSc. (Phys.-Math), **SPIN-code: 9569-5642**, **ResearcherID: Q-4144-2016**, **ORCID ID: 0000-0003-0949-2040**, **Scopus Author ID: 57205741734**, darik777mhi-ras@mail.ru

Contribution of the co-authors:
Vladimir V. Efimov – task setting, formulating conclusions

Darya A. Iarovaia – performing conclusions, interpreting simulation results, participating in the discussion of simulation results and formulating conclusions

The authors have read and approved the final manuscript.
The authors declare that they have no conflict of interest.